#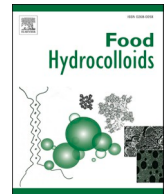 Printability and interfacial performance of emulsion gels and bigels in multi-material dual and coaxial food 3D printing

(article starts on next page)

Printability and interfacial performance of emulsion gels and bigels in multi-material dual and coaxial food 3D printing

Linnea Johansson [a], Isabel Badager [a], Annika Krona [b], Mehdi Abdollahi [b,*]

[a] *Department of Life Sciences-Food and Nutrition Science, Chalmers University of Technology, Kemigården 4, Gothenburg, SE-41296, Sweden*
[b] *RISE Research Institutes of Sweden, Agriculture and Food, Box 5401, 402 29, Gothenburg, Sweden*

ABSTRACT

Structured fats like emulsion gels and bigels have emerged as promising animal fat substitutes for plant-based meat analogs. This study investigated the printability, rheological behavior, and interfacial compatibility of emulsion gels and bigels in combination with pea protein isolate (PPI) for extrusion-based single- and multi-material dual and coaxial 3D food printing (3DFP). Rheological analysis confirmed that despite having both systems exhibiting shear-thinning and thixotropic behavior, bigels demonstrate higher mechanical strength (G' = 1000 Kpa vs 10 Kpa) and structural integrity (yield stress = 500 Pa vs 200 Pa). These properties translated into better print fidelity, with bigels maintaining defined structures across a range of temperatures (30–60 °C) in single-material 3DFP while emulsion gels were prone to phase separation, deformation and collapsing. In multi-material 3DP with PPI, bigels consistently demonstrated clear material separation, forming distinct core-shell structures in coaxial setups as well as maintaining well-defined, evenly distributed phases in dual extrusion. In contrast, emulsion gels exhibited smearing, irregular distribution, and poor interfacial definition in both setups, indicating weaker phase stability and compatibility with the protein matrix. Confocal laser scanning microscopy confirmed better interfacial phase boundaries between bigels and PPI, aligning with rheological and printing outcomes. In conclusion, bigels show high promise as multi-functional structuring agents and fat substitutes in multi-material 3DFP, while emulsion gels require further optimization to enhance their print performance and material compatibility.

1. Introduction

The demand for plant-based meat alternatives is increasing due to the growing awareness of environmental sustainability, ethical concerns, and health considerations. However, one of the key challenges in developing these products lies in achieving the sensory attributes comparable to real meat, including texture, mouthfeel and juiciness (Appiani et al., 2023; Szenderák et al., 2022). Although significant progress has been made in replicating the fibrous protein-based structure of meat, the role of fats has often been overlooked, despite their critical importance to overall sensory acceptance (Bajželj et al., 2021; Villacís-Chiriboga et al., 2025). The challenge in replacing animal fats stems from fundamental differences in physical state and functional prnaziroperties compared to plant-based lipids. Animal fats are typically solid at room temperature, contributing to the structural cohesion and rich mouthfeel of meat, while plant-based oils are liquid, leading to markedly different mechanical and thermal behaviours (Chen et al., 2023). These

differences significantly affect the structural integrity, sensory quality, and ultimately the consumer acceptance of plant-based meat analogs (Chen et al., 2023).

To address this challenge, structured fat systems such as emulsion gels and bigels have emerged as promising candidates for application in plant-based meat products. Emulsion gels consist of an emulsion phase embedded in a gel network, combining the stability of gels with the functional benefits of emulsions (Cen et al., 2024). Bigels, on the other hand, are emerging biphasic systems composed of both a hydrogel and an oleogel, combining the properties of both phases (Chao et al., 2024). These systems offer enhanced mechanical stability and improved viscoelastic properties, making them an attractive candidate for structured fat applications. Additionally, they can be tailored to optimize texture, mouthfeel, and flavour release, facilitating their use in a wide range of plant-based food products (Chao et al., 2024; Czapalay & Marangoni, 2024). Despite the reported advantages of both structured fat systems, there is a notable lack of comparative studies evaluating

* Corresponding author.
  E-mail address: khozaghi@chalmers.se (M. Abdollahi).

their performance as fat mimetics in meat analogs.

In recent years, food 3D printing (3DP) has gained attention as a versatile technique for creating complex food structures, especially in meat analogs (Wen et al., 2023). This technology enables precise control over the composition, structure, and appearance of the final product, making it possible to replicate intricate features such as the spatial distribution of fat, most notably, the marbling seen in conventional meat products (Cen & Meng, 2024). Multi-material 3D printing (MM3DP) further extends this capability by enabling the simultaneous deposition of multiple components, such as structured fats and protein matrices, through techniques like dual extrusion, where two materials are deposited side by side, and coaxial extrusion, where one material is encapsulated within another with a common longitudinal axis (see Fig. 1) (Caron et al., 2024; Y. Wang et al., 2025). However, the effective application of structured fat systems in MM3DP introduces additional complexity and depends on a fine-tuned balance of properties, including rheological behavior, extrudability, thermal stability, and interfacial compatibility with other printed phases (Tang et al., 2024). These requirements highlight the need to understand how different fat mimetics perform under 3DP conditions and how their physical and functional characteristics influence print fidelity, structural integrity, and ultimately, the quality of the final product.

Emulsion gels and bigels have been individually investigated as fat mimetics, proving their viability in food 3D printing (Cen & Meng, 2024). Emulsion gels have demonstrated favorable rheological properties, shape fidelity, and extrudability, making them suitable candidates for 3D-printed fat phases. Studies have shown that emulsion gels can mimic the texture and mouthfeel of animal fats, and their application in 3D printing has been explored for developing reduced-fat meat analogs (Cen et al., 2024; Liu et al., 2025; Zhong et al., 2024). Similarly, bigels offer unique structural and rheological advantages that can be effectively tailored, such as thermal stability and controlled phase distribution, which have been leveraged in recent food 3D printing studies (Qiu

et al., 2022, 2024; Sinha et al., 2024). Bigels have been studied for their potential to encapsulate and deliver bioactive compounds, and their gel-like consistency makes them suitable for extrusion-based 3D printing (Chao et al., 2024; Sinha et al., 2024). While both systems have been explored as fat analogs, their performance in MM3DP, particularly in combination with protein-based matrices, remains largely unaddressed. To the best of our knowledge, no studies have systematically evaluated their side-by-side performance as structured fat substitutes in MM3DP. There is limited understanding of how these systems behave under different extrusion techniques, including dual and coaxial extrusion. Additionally, their compatibility with plant protein matrices has not been systematically tested in this context. Addressing these gaps is critical for optimizing the performance of structured fats in food 3DP and for advancing the development of realistic, high-quality plant-based meat analogs.

The present study aimed to systematically evaluate the potential of emulsion gels and bigels as structured fat substitutes for application in MM3DP. Specifically, the objectives were to: (1) conduct a side-by-side comparison of emulsion gels and bigels as animal fat mimetics in extrusion-based food 3D printing, including their rheological and microstructural properties; (2) assess their compatibility and performance in MM3DP alongside a pea protein isolate-based food ink with particular attention to interfacial microstructure; and (3) investigate the influence of dual and coaxial extrusion techniques on the printability of both fat systems within MM3DP setups.

2. Materials and methods

2.1. Materials

A commercial pea protein isolate called NUTRALYS® F85M, from Roquette, France, with a protein content of 66.70 ± 0.12 % (calculated with a conversion factor of 5.4), was used. All polysaccharides, xanthan
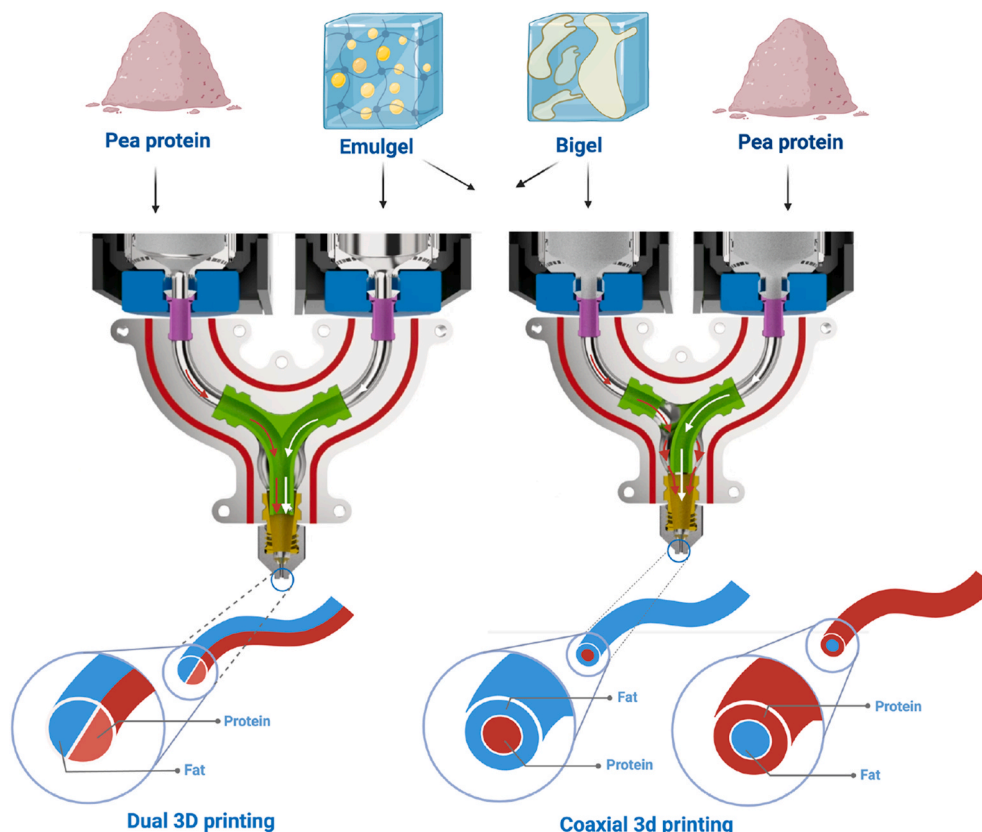

Fig. 1. Schematic view of the dual and coaxial 3D printing module and resulting printing of multi-material fibers.

gum (CAS: 11188-66-2), κ-carrageenan (CAS: 11114-20- 8) and agar (CAS: 9002-18-0) as well as beeswax (CAS: 8012-89-3) and citric acid (CAS: 5949-29-1), were purchased from Sigma-Aldrich. Rapeseed oil (EXTRA) was bought from a local store called Coop.

2.2. Study design

The study was designed in two steps to evaluate the potential of emulsion gels and bigels as animal fat mimics for MM3DP. In the first step, the two gels were subjected to a side-by-side comparison in single-material 3D printing to assess their printability and shape-retention behavior and their underlying rheological and microstructural drivers. Both gels were prepared following standardized protocols previously reported for their single-material 3D printing to ensure reproducibility and comparability, and their functional performance was characterized by rheological and microscopic analyses. This enabled a direct assessment of how their distinct internal architectures contribute to printability and suitability as animal fat mimics. In the second step, the gels were evaluated in MM3DP together with pea protein isolate, using dual/mixed deposition as well as coaxial printing to create structured lines. The resulting interfacial interactions between the gels and the protein matrix were examined using confocal laser scanning microscopy (CLSM). This two-step approach provided a systematic comparison of the structural and interfacial performance of the two gel systems under conditions relevant to fat–protein hybrid architectures.

2.3. Preparation of emulsion gel

The emulsion gel was prepared according to the method described by Zhu et al. (2024) to ensure the emulsion gel's individual 3D printability, with some modifications. Briefly, 15.7 wt% pea protein isolate (PPI) and 2 wt% agar were dissolved in distilled water and its pH was adjusted to 3.4 by adding citric acid. The addition of agar was targeted to enhance the gel's viscoelastic properties. The protein solution was then mixed with 40 ml of rapeseed oil using an Ultra-Turrax at 20,000 rpm for 2 min to form the emulsion. The emulsion was subsequently heated at 80 °C for 30 min in a shaking water bath (Julabo, SW22) to induce gel formation, followed by direct transfer to a stainless steel 3D printing cartridge. The cartridge was placed on ice for 30 min before being stored overnight at 4 °C. All subsequent tests were performed the following day.

2.4. Preparation of bigel

The bigel was prepared according to the method described by Qiu et al. (2022) based on their formulation with the best 3D printability. To prepare the hydrogel, a 1:1 ratio of κ-carrageenan and xanthan gum was added to distilled water at a total concentration of 1.5 wt%. The mixture was heated at 99 °C in a shaking water bath (Julabo, SW22) for 40 min while stirred at 200 rpm for 40 min. The oleogel was formed by dissolving 15 wt% beeswax in rapeseed oil, followed by heating at 80 °C and stirring it at 200 rpm for 40 min in the water bath. Both gel phases were kept in the water bath at 99 °C to maintain their fluid state.

To form the bigel, the hydrogel and oleogel phases were combined and homogenized at 80 °C using an Ultra-Turrax at 15,000 rpm for 2 min. The resulting bigel was immediately transferred to a cartridge, cooled on ice for 30 min, and then stored overnight at 4 °C. All subsequent analyses were performed the following day.

2.5. Preparation of pea protein isolate ink

The pea protein isolate-based ink was prepared by dispersing 30 wt% PPI and 0.5 wt% red food coloring (to resemble the appearance of meat) in distilled water and mixing using a portable food chopper for 30 min as described by Sajib et al. (2023). For samples intended for confocal laser scanning microscopy (CLSM), food coloring was omitted to avoid interference with the fluorescent staining. The mixer was then sealed

and left to completely hydrate for 1 h before loading into the cartridges. The prepared ink was immediately used for 3DP.

2.6. Rheological analysis

Rheological measurements were performed using the Paar Physica MCR 300 Rheometer (Anton Paar GmbH, Austria) equipped with a 25 mm parallel plate geometry (PP25) and 1 mm gap as explained by Abdollahi et al. (2025). All samples were tested at 25 °C unless otherwise stated, with duplicate measurements.

An amplitude sweep (0.01–1000 % strain at 10 rad/s) was conducted to determine the linear viscoelastic region (LVR). A shear viscosity test was conducted by varying the shear rate from 0.001 to 100 1/s, to evaluate the materials' shear-thinning behaviour. Frequency sweep tests were varied between 200 rad/s and 0.1 rad/s at 0.01 % strain within the LVR to measure the storage modulus (G') and loss modulus (G"). Thixotropic behaviour was assessed using a three-interval thixotropy test (3ITT) with shear strains of 0.01 % (200 s), 10 % (100 s) and lastly 0.01 % (200 s) with an angular frequency of 10 rad/s. Temperature sweeps were carried out from 4 °C to 80 °C and then cooled back to 4 °C at a rate of 5 °C/min to evaluate the thermal reversibility of the gels. The rheological data were plotted and statistically analyzed using MATLAB R2022b. For each test, the mean and standard deviation were calculated for all replicates.

2.7. 3D printing

2.7.1. Single-material 3D printing

3D printing was performed using a dual-head extrusion-based printer developed in collaboration with FELIXPrinters and Chalmers University of Technology. The printer was equipped with a custom-designed mixing module (see Fig. 1), which enables switching between dual and coaxial extrusion. Printing models included a rectangular hollow tube (height of 20 mm and a width of 23.6 × 23.6 mm) developed and sliced using 3D Slicer software. For all tests, the extrusion multiplier was set to 1.25.

For single-material 3DP, a 1.0 mm nozzle was used with an extrusion width of 1.80 mm, a layer height of 0.80 mm, a first layer height of 1.00 mm and a first layer width of 0.60 mm. The printing speed was set to 25.0 mm/s with a first layer speed of 15.0 mm/s. Retraction settings included a retract distance of 1.00 mm, a retract speed of 5.00 mm/s, an extra restart distance of −0.05 mm, a coasting distance of 3.00 mm, and a wiping distance of 3.00 mm. To evaluate the effect of temperature on printability, the printing temperature was varied by adjusting the extruder temperature to 30, 40, 50, and 60 °C for both the emulsion gel and the bigel formulations.

2.7.2. Multimaterial dual and coaxial 3D printing

For MM3DP, one extruder contained a stainless steel cartridge filled with pea protein isolate ink and the other extruder contained a stainless steel cartridge filled once with the emulsion gel and once with the bigel. For dual extrusion, the layer height and extrusion width were set to 4.0 mm, with a printing speed of 25.0 mm/s, and the same retraction and coasting parameters as in single-material printing. A 4.0 mm nozzle was used to provide a clearer observation of the distribution between the materials within the extruded strand, allowing for better assessment of material compatibility. This evaluation was performed using a line test to assess the distribution of the two materials along the extruded strand. Before the line test, a purge cube was printed to ensure the correct material ratio had been adjusted, allowing the materials to reach a stable flow and consistent distribution before the main evaluation. For coaxial extrusion, the strands were slowly extruded to ensure a round shape, clearly revealing the distribution between the core and the surrounding material. The printing temperature was room temperature for the emulsion gel and pea protein isolate, and 40 °C for the bigel, based on the results obtained in the single-material 3D printing at various

temperatures.

2.8. Confocal laser scanning microscopy (CLSM)

The microstructure and phase distribution of the emulsion gel and bigel during single material 3DP and the interface of the two materials with pea protein in MM3DP were analyzed using a Leica SP5 confocal laser scanning microscope (CLSM) (Leica Microsystems GmbH, Germany) equipped with the objectives HC PL FLUOTAR 10.0×0.30 DRY and HCX PL APO lambda blue 20.0x0.70 IMM UV and used in inverted mode. Protein and hydrogel phases were stained with fluorescein iso-thiocyanate (FITC), shown in green, and lipids with Nile Red, shown in green. Samples were prepared by placing small sections of the gels on glass coverslips. No additional preparation was required beyond staining. FITC (green spectrum) was excited at 488 nm with emission collected between 500 and 520 nm, while Nile Red (red spectrum) was excited at 488 nm and captured at 570–610 nm. Micrographs were captured with a resolution of 1024x1024 and 8 lines average.

2.9. Photographic documentation

The objects were photographed in a portable mini studio (Foldio3, ORANGE- MONKIE Inc) against a white background. The cut segments of the extruded strands in the coaxial extrusion analysis were photographed against a blue background to enhance visibility. All images were captured using an iPhone 12 Pro.

2.10. Statistical analysis

Statistical analysis was performed using SPSS software (IBM Corp. Released 2021. IBM SPSS Statistics for Macintosh, Version 28.0. Armonk, NY: IBM Corp). The rheological data was evaluated using a one-way analysis of variance (ANOVA) followed by Duncan's multiple range test to determine significant differences between groups. All statistical analyses were performed with a significance level of 0.05, where differences of $p < 0.05$ were considered significant.

3. Results and discussion

3.1. Rheological properties

Rheological properties are critical for successful 3DP, as they determine the material's ability to flow through the nozzle, maintain shape upon deposition, as well as support subsequent layers without collapsing. These features directly impact the print quality and structural integrity of the final product (C. Wang et al., 2023).

As can be seen in Fig. 2, both the emulsion gel and bigel formed stable structures capable of supporting their own weight during the inversion test, confirming their solid-like behavior at room temperature. The amplitude sweep results (Fig. 3a and Supplementary Fig. 1, Table 1) revealed that the bigel had a significantly higher storage modulus (G') across the LVR range, indicating a more rigid and elastic network, but with a narrower LVR region in the strain sweep and the higher yield stress (see Supplementary Fig. 1) compared to the emulsion gel. This implies a higher resistance to structural breakdown but with low deformability, meaning that bigel behaved as a strong gel at small deformations but is more brittle or fragile when deformation increases and it was more solidified (Shakeel et al., 2021). In contrast, the emulsion gel maintained a broader LVR range, showing a more flexible, but potentially less mechanically stable, network.

The yield strain was significantly ($p < 0.05$) higher for the emulsion gel (8.4 %) compared to the bigel (0.99 %) but its yield stress was lower (238 kPa vs 515 kPa), due to its wider LVR, indicating that a greater applied deformation is necessary to initiate a flow. These observations are consistent with previous reports, where bigels composed of structured oleogels and hydrogel matrices often showed higher elastic moduli due to the reinforcing effect of the solid lipid phase (Qiu et al., 2022). However, the narrower LVR observed here may reflect reduced structural resilience, as also noted by (Zampouni et al., 2024), that highly elastic bigels tend to fracture more easily under shear. In contrast, emulsion gels, which are often stabilized by proteins and polysaccharides, typically demonstrate higher yield stress and broader LVR, enabling better recovery after deformation (Hashemi et al., 2025). These rheological traits suggest that while bigels may offer enhanced structural rigidity, emulsion gels may provide better resistance to mechanical disruption during extrusion and printing, making them potentially more robust candidates for continuous layer-by-layer deposition in 3D printing.

Both gels exhibited shear-thinning behaviour, characterized by a reduction in viscosity with increasing shear rate, as shown in Fig. 3b. The bigel demonstrated a higher initial viscosity compared to the emulsion gel, indicating a denser internal structure, but also a steeper decline, indicating stronger shear-thinning properties. This is advantageous for 3DP as it supports smooth extrusion and rapid solidification upon deposition but requires higher extrusion forces (Torres, 2017). Similar trends have been observed in other bigel systems where wax-based oleogels are incorporated, contributing to high yield stress and strong structural rigidity under low shear conditions (Qiu et al., 2022, 2024).

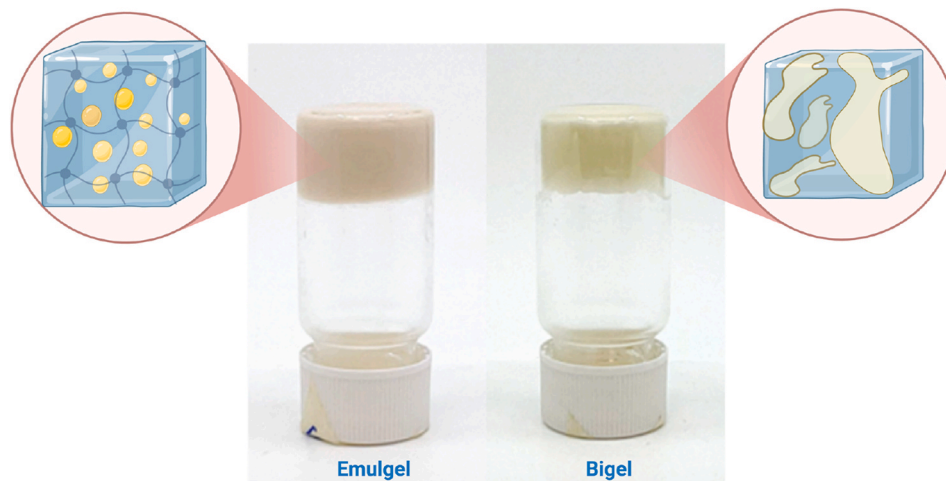The frequency sweep (Fig. 3c) confirmed that both gels maintained a

Fig. 2. Visual representation of the tube inversion test and schematic microstructure of emulsion gel and bigel.
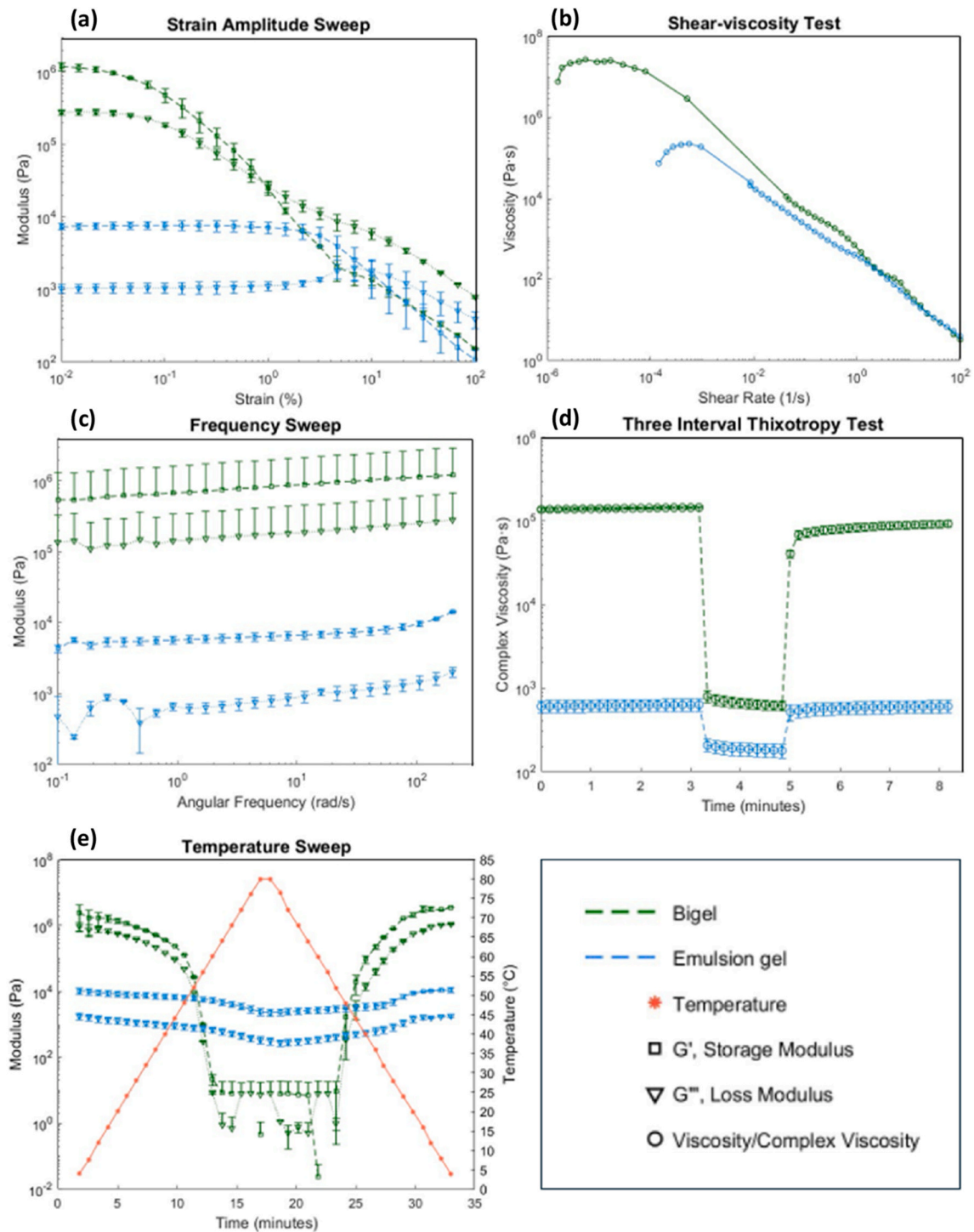
Fig. 3. Rheological properties of emulsion gel and bigel formulations, including changes in their storage (G′) and loss modulus (G″) during (a) amplitude sweep, (b) shear viscosity test or flow curve, (c) frequency sweep, (d) three interval thixotropy test: Changes in complex viscosity over three intervals, and (e) temperature sweep.

Table 1
Rheological parameters of the emulsion gel and bigel developed as 3D printing ink.

Sample	Zero shear viscosity (kPa.s)	Storage modulus (kPa)	Yield stress (Pa)	Yield strain (%)	Complex viscosity at 1st interval of 3ITT (kPa.s)	Complex viscosity at 3rd interval of 3ITT (kPa.s)
Emulsion Gel	125 ± 18.34[b]	7.39 ± 0.74[b]	238.5 ± 50.91[b]	8.41 ± 2.24[a]	0.60 ± 99.5[a]	0.58 ± 130.8[a]
Bigel	19800 ± 7956[a]	1200 ± 155.56[a]	515.5 ± 115[a]	0.99 ± 0.0007[b]	137.2 ± 6.5 [a]	68.1 ± 8.90 [a]

Different small letters in each column show significant differences.

higher G′ compared to G″ across the frequency range, indicative of predominantly solid-like behaviour. The bigel exhibited a significantly higher G′, suggesting a more structurally integrated, elastic internal network. No crossover points were observed. However, the emulsion gel exhibited a small dependency on higher frequencies, which suggests that it has a softer nature than the bigel. Previous studies have also reported that emulsion gels stabilized by protein–polysaccharide matrices tend to exhibit lower rigidity but better deformation tolerance, making them potentially more resilient during printing (Hashemi et al., 2025).

The 3ITT profiles in Fig. 3d showed that both gels exhibit thixotropic behavior. The complex viscosity was consistently higher for the bigel across all intervals, indicating a stronger resistance to flow at rest. With increased shear strain, both gels displayed a sharp decrease in complex viscosity, aligning with the shear-thinning behaviour observed in the shear viscosity test. Both gels demonstrated quick recovery after decreasing the applied strain but none of the gels showed a complete recovery upon relaxation, indicating irreversible structural breakdown to some extent. Interestingly, the emulsion gel showed a slightly faster recovery rate compared to the bigel, suggesting a more dynamic and adaptable microstructure. This aligns with prior findings that protein–polysaccharide-stabilized emulsion gels can exhibit rapid but partial network rebuilding due to reversible physical interactions (Dickinson, 2012; Hashemi et al., 2025). In contrast, the stronger, more interconnected structure of bigels, often involving crystalline wax or gelator domains, tends to resist reformation once disrupted, as also reported in other bigel-based studies (Gu et al., 2023; Qiu et al., 2024; Zampouni et al., 2024).

Temperature sweeps (Fig. 3e) indicated that the emulsion gel maintained a relatively stable G′ across the tested temperature range (4–80 °C), reflecting its high thermal stability and resistance to heat-induced structural degradation. The thermal stability of the emulsion gel can be attributed to the combined effects of heat-induced pea protein aggregation and the thermally stable agar network. Upon heating, denatured pea proteins form a cohesive interfacial layer around the oil droplets and aggregate into a viscoelastic matrix, while the agar hydrogel retains its gel integrity, resulting in a reinforced composite network resistant to thermal deformation.

In contrast, the bigel exhibited a sharp drop in G′ around 50 °C, reflecting the melting of the oleogel phase, followed by a plateau between 60 and 80 °C, suggesting partial structural stabilization, likely maintained by the hydrogel network. After cooling back to around 20 °C, both moduli recovered closely to their initial values, indicating significant recovery of the bigel, thereby showing its good thermal reversibility. These findings highlight the differences in thermal stability between the gels. The emulsion gel appears more thermally stable, whereas the bigel, on the other hand, is more responsive to temperature changes, which might facilitate smoother extrusion at elevated temperatures. These results emphasize key functional differences between the gels. The thermal stability of the emulsion gel is likely attributed to the protein-polysaccharide matrix, which is less sensitive to moderate heating (Hashemi et al., 2025). Similar behavior has been reported for protein-based emulsion gels stabilized by carrageenan or starch (Asyrul-Izhar et al., 2023; Xiong et al., 2022). The thermal sensitivity of the bigel is consistent with the melting of the beeswax oleogel phase around 50–60 °C, as previously described (Gu et al., 2023; Vershkov & Davidovich-Pinhas, 2023).

From a fat mimetic perspective, these thermal behaviors have important implications. Animal fats typically begin to melt between 30 and 50 °C, contributing to meat juiciness and mouthfeel upon cooking. The sharp but reversible softening of the bigel around this range suggests it could effectively mimic the thermal phase transition of animal fats during heating, releasing oil in a manner akin to natural fat melting (Hanbeyoglu-Akturk et al., 2025). Meanwhile, the thermal stability of the emulsion gel may be advantageous for applications requiring structural retention during extended or high-temperature processing, though it may lack the dynamic melt-release behavior characteristic of animal fats. These functional differences may guide tailored applications in 3DP of meat analogs where fat retention or controlled melting is desirable.

The emulsion gel was prepared according to the method reported by Zhu et al. (2024), who observed thermal reversibility in their emulsion gel. One possible reason for this variation is the significant difference in protein purity. The PPI used in this study had a protein content of 66.7, compared to the 96.1 reported (Zhu et al., 2024). This lower protein purity likely impacted the protein network formation and the ability to form reversible hydrogen bonds, both of which are critical for achieving thermal reversibility in protein-based gels. However, the other rheological properties observed for the emulsion gel aligned with their results, indicating that the lower protein purity likely affected only the thermal reversibility. The results regarding the bigel in this study aligned well with those reported by Qiu et al. (2022). However, it is important to note that they did not perform temperature sweeps to specifically evaluate the thermal reversibility of their bigel formulations.

3.2. Single-material 3D printing performance of emulsion gel vs bigel

The single-material 3DP performance of the emulsion gel and bigel was evaluated to assess their extrudability, buildability and overall print quality.

To investigate the effect of extrusion temperature on 3D printability, both emulsion gel and bigel formulations were printed at 30 °C, 40 °C, 50 °C, and 60 °C. Representative frontal, side, and top views of the printed structures are shown in Fig. 4.

At 30 °C, the emulsion gel exhibited relatively good printability, characterized by some inconsistent layer deposition and minor deformation at the base. At 40 °C, a substantial improvement in shape fidelity and structural uniformity was evident. The gel demonstrated smoother walls and consistent layer deposition, indicating improved flowability and reduced viscosity under shear. Moderate heating facilitates partial weakening of internal gel structures (e.g., protein or polysaccharide networks), enhancing their deformation and yielding behavior without undermining self-support (Pulatsu & Lin, 2021). This balance is crucial in extrusion-based 3D printing, where the material must be flowable through the nozzle but sufficiently firm to retain shape upon deposition. However, at 50 °C, the structural quality began to deteriorate. The layers showed early signs of sagging and spreading, particularly in the top regions. At 60 °C, this effect was more pronounced: over-extrusion, bulging at the edges, and collapse of upper layers became evident. This decline in printability can be attributed to over-softening of the emulsion matrix, leading to reduced yield stress and impaired self-support (Jiang et al., 2019; Outrequin et al., 2023). As the gel transitions from a viscoelastic solid to a more fluid-like state, it loses the mechanical resistance necessary to retain printed architecture. These results align with studies showing that temperature plays a dual role in gel extrusion—facilitating flow yet potentially undermining buildability when excessive (Lille et al., 2018; Outrequin et al., 2023)

For the bigel formulation, 30 °C printing led to visible instability in extrusion. The printed structures were rough with poorly defined walls, suggesting that the gel was too stiff for smooth flow and consistent layer deposition. At 40 °C, optimal printability was achieved. The bigel demonstrated excellent extrudability with sharp edges, uniform walls, and stable stacking. This suggests that 40 °C facilitated just enough softening of the gel phases (oleogel and hydrogel), promoting flowability while preserving the structural memory essential for shape retention (Fernandes et al., 2023; Qiu et al., 2022). At 50 °C, however, the print quality began to decline. The layers showed bulging and uneven flow, with early signs of structural deformation. This suggests that the bigel lost part of its viscoelastic strength, possibly due to weakened interfacial interactions or breakdown in the bicontinuous network. At 60 °C, these effects worsened, leading to significant roughness in the texture of the printed walls, making the printed structure unsuitable.
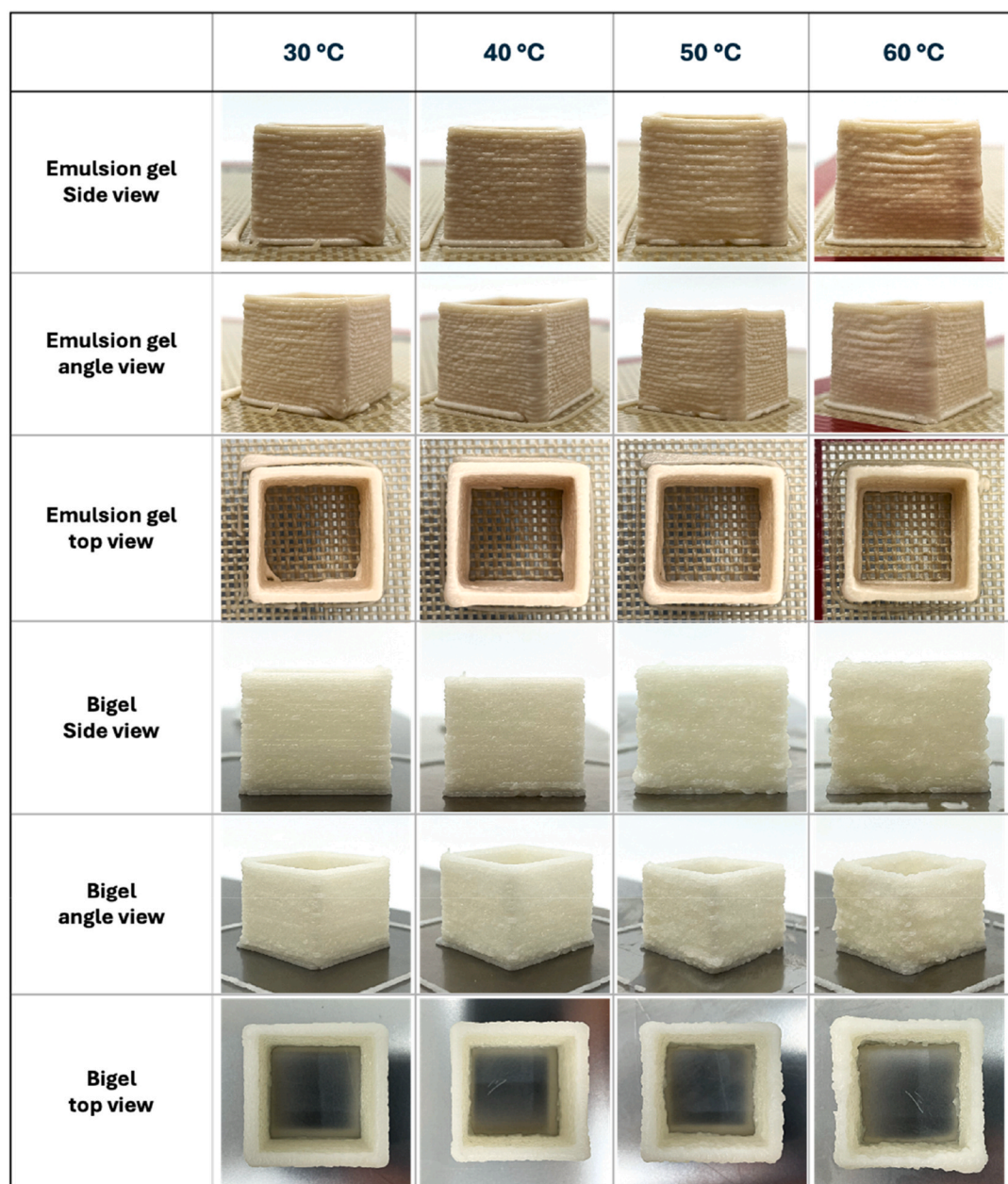
Fig. 4. Visual appearance of objects from emulsion gel and bigel printed at four different temperatures of 30 °C, 40 °C, 50 °C, and 60 °C. The object printed at each temperature is shown from the side, angle and top view.

Bigels are known for their temperature-responsive viscoelastic behavior, where moderate heating improves flowability but excessive heat compromises internal structure (Fernandes et al., 2023; Zampouni et al., 2024). The biphasic nature of bigels means their stability depends on the mechanical interplay between the hydrogel and oleogel phases, which can be disrupted at higher temperatures.

Both the emulsion gel and bigel exhibited a temperature-dependent window of optimal printability, but with distinct behavior. While the emulsion gel performed best at 40 °C, the bigel showed superior print quality at 50 °C. This divergence reflects their compositional and structural differences: emulsion gels rely on finely dispersed oil droplets within a continuous aqueous matrix, whereas bigels are biphasic systems combining oleogels and hydrogels, often resulting in higher thermal stability and modified rheological properties. These findings underscore the importance of temperature control during extrusion-based 3D food printing. Maintaining an optimal thermal range is essential to achieve the necessary balance between flowability for

extrusion and firmness for structural retention. In line with previous studies (Lille et al., 2018), our results show that small changes in extrusion temperature can have large effects on print fidelity, emphasizing the need for formulation-specific printing protocols. In this study, the emulsion gel formulation was able to successfully print taller structures than those previously reported by (Zhu et al., 2024). While they primarily focused on prints with lower height, the formulation used here demonstrated sufficient mechanical strength and structural integrity to support greater heights. This enhanced printability likely reflects improvements in internal network stability, potentially due to the inclusion of agar, which possesses strong gel-forming abilities.

The 3DP performance of bigel is consistent with the findings of (Qiu et al., 2022) who identified several key factors contributing to the successful 3D printability of bigels. They noted that its composition of hydrogel-to-oleogel (20:80) provides suitable consistency and fluidity for smooth extrusion without clogging, as well as it exhibiting rapid recoverability to retain structural stability after extrusion and strong

mechanical properties to support complex printed shapes.

To further evaluate the self-supporting performance, taller structures were printed. As shown in Fig. 5a, the emulsion gel demonstrated moderate buildability. At lower heights (e.g., 10–20 layers), the printed structures retained good geometric fidelity, with well-aligned walls and defined edges. However, as the number of layers increased, the structure began to exhibit progressive deformation, particularly at the base and top. This deformation likely results from the gradual accumulation of compressive stress on the lower layers, leading to lateral spreading and collapse. The emulsion gel's failure at higher layers is consistent with known challenges in extrusion-based 3D food printing, where materials with insufficient yield stress or elastic recovery cannot support increasing vertical loads (Godoi et al., 2016; Qiu et al., 2024). Although emulsion gels typically benefit from internal oil droplet networks that improve viscoelasticity, the balance between flowability and stiffness must be finely tuned. When too soft, they deform; when too rigid, they hinder extrusion.

In contrast, the bigel, Fig. 5b, showed superior buildability. Printed structures maintained their shape even at increased layer heights, with minimal distortion but with decreased resolution at elevated layers heights. Walls remained vertical and interlayer boundaries nearly aligned throughout stacking, suggesting that the bigel had a more robust internal architecture capable of withstanding vertical pressure. This better performance can be attributed to the biphasic network of the bigel, combining an oleogel and a hydrogel phase, providing both mechanical strength and structural resilience (Fernandes et al., 2023; Hanbeyoglu-Akturk et al., 2025). The interpenetrating or bicontinuous nature of the gel phases likely enhanced the overall yield stress and viscoelastic moduli, which are critical for load-bearing applications in 3D food printing (Zampouni et al., 2024). When the printed object's height exceeded a certain threshold, surface roughness became apparent in the bigel layers. This is a common issue with shear-thinning materials that have a relatively slow setting or solidification rate. As the object grows taller, the weight of the upper layers can deform the lower ones, leading to increased layer height and instability. Consequently, the upper layers experience excessive stress relaxation after deposition, resulting in a rough surface texture. This issue can be mitigated by optimizing printing parameters or modifying the material formulation to better support the desired geometry and height.

While both systems are printable under the tested moderate conditions, bigel outperformed the emulsion gel in buildability in taller objects, demonstrating that internal gel architecture critically affects the material's ability to sustain its weight and retain precise shapes in vertical builds. This aligns with the rheological data, where the bigel exhibited a narrower LVR but higher G′, indicating a stiffer network. This is particularly important in food printing where complex, multi-layered structures are desirable for sensory and functional reasons but also for MM3D, where the material should be able to be printable together with other materials, imposing extra stress. The emulsion gel also displayed faster phase separation and lower storage stability (see Supplementary Fig. 2). Additionally, the self-supporting properties of bigel were confirmed by placing printed objects on their sides without deforming, maintaining their shape despite lacking support from underlying layers (Supplementary Fig. 2). The structure is even able to withstand additional weight without deforming, further highlighting the superior mechanical stability of the bigel. These findings suggest that bigel is better suited for more structurally demanding single-material 3DP applications.

3.3. Confocal laser scanning microscopy (CLSM) of single-material 3DP

CLSM was used to evaluate the microstructure of the emulsion gel and bigel before and after single-material 3DP. The micrographs revealed significant differences in phase distribution and structural stability between the two systems.

In the emulsion gel, CLSM micrographs (Fig. 6) showed a dispersed oil-in-water (O/W) structure, with lipid-rich oil droplets distributed within a continuous protein-rich hydrogel phase, which was expected due to the ratio of the phases. However, the droplets appeared unevenly distributed and often clustered together, indicating partial phase separation and a weaker internal structure. This aligns with the faster phase separation observed in storage tests (Supplementary Fig. 3). The protein matrix appeared as bright green regions that were not uniformly dispersed, suggesting poor emulsification and weaker network stability, consistent with the lower G' observed in the rheological analysis. This was also aligned with the 3DP performance, as the emulsion gel collapsed under increased layer height. Compared to the findings in the study of Zhu et al. (2024), the emulsion gel in this study appears less stable when looking at CLSM results, which may be due to the variations in PPI composition between the studies.

In contrast, the bigel displayed a water-in-oil (W/O) structure characterized by a continuous oleogel matrix with smaller, well-dispersed hydrogel clusters, see Fig. 6, and was expected due to the high ratio of oleogel compared to hydrogel. This structure remained
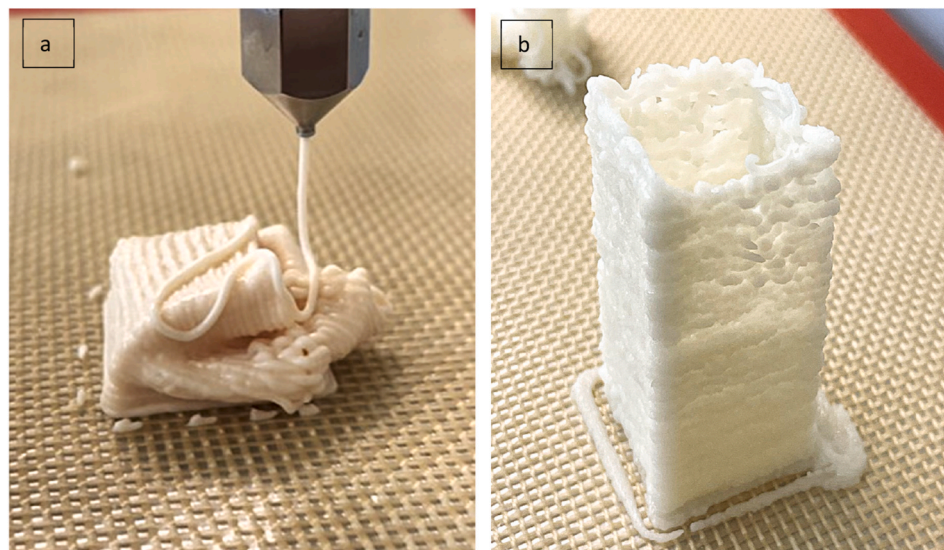

Fig. 5. 3D printing evaluating increased layer height as a part of a pre-study to evaluate the buildability of the gels. (a) Emulsion gel and (b) bigel. This modification potentially broadens the application range of emulsion gels in food 3DP.
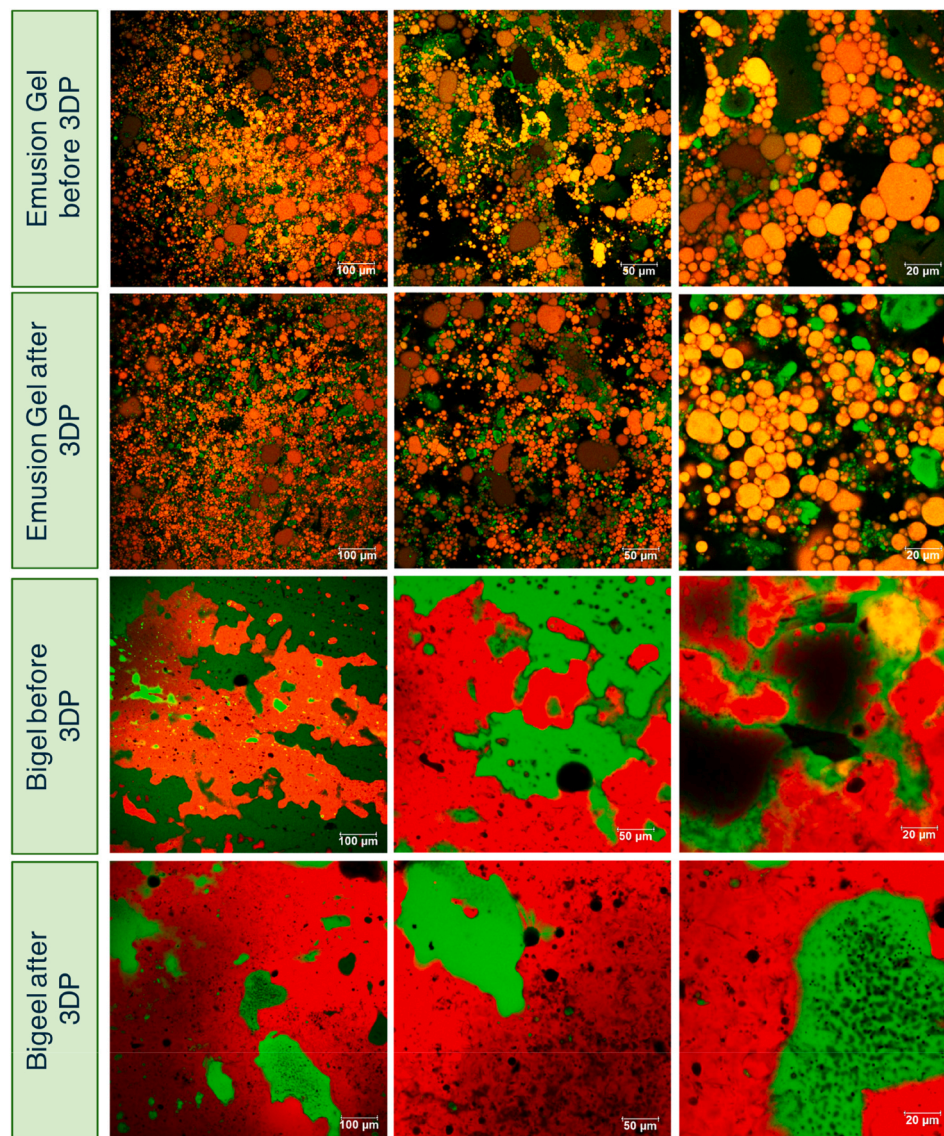
Fig. 6. Confocal laser scanning microscopy (CLSM) micrographs of emulsion gel and bigel, captured before and after 3D printing (3DP) at three different magnifications with scale bars representing 100 μm, 50 μm, and 20 μm from left to right. Protein and hydrogel in green, oil and oleogel in red. (For interpretation of the references to color in this figure legend, the reader is referred to the Web version of this article.)

stable after 3DP, with no visible changes in droplet size or distribution, indicating strong phase stability and structural recovery. The inter-penetrating gel phases appeared resilient to the shear forces during extrusion, likely due to their higher mechanical strength and inter-connected nature, which provided sufficient recovery upon deposition. These findings are also consistent with the rheological results, where the bigel exhibited a higher storage modulus and stronger gel network, contributing to its superior mechanical stability. A similar observation was reported by Qiu et al. (2022), who connected the ability to maintain a stable microstructure during printing to the quick recovery characteristics and highly ordered structure of bigel.

3.4. Multi-material 3D printing performance of emulsion gel vs bigel

MM3DP was performed to assess the compatibility of the gels with pea protein isolate when printed in dual and coaxial configurations. In dual extrusion, the emulsion gel struggled to maintain a consistent 50:50 distribution, exhibiting smearing and blending with the protein matrix, as shown in Fig. 7b. The smearing further confirms the weaker gel network of the emulsion gel revealed in the rheological properties

assessment by its lower storage modulus (G′), with insufficient mechanical integrity to form and retain discrete layers under extrusion stress. Smearing was mitigated at reduced extrusion speeds (Fig. 7c), suggesting that lower shear rates allow more time for material deposition and recovery, thus improving spatial resolution. However, even at optimized speeds, the emulsion gel displayed random co-ejection alongside the protein phase, indicating low cohesiveness and possible slippage in the feeding mechanism, typical of systems with insufficient yield stress or structural rigidity (Jiang et al., 2019; Lille et al., 2018; Outrequin et al., 2023)

In contrast, the bigel formulation demonstrated superior strand definition and sharper phase boundaries, indicating better compatibility with pea protein phase during dual printing. Although minor irregularities were visible at higher speeds, the bigel exhibited clearer layer separation and less blending, attributed to its interpenetrating gel network that resists deformation and provides structural support under shear (Lille et al., 2018; Patel, 2017). The biphasic architecture of bigels, combining an oleogel and a hydrogel, offers greater internal cohesion and viscoelastic recovery, both of which are crucial for successful MM3DP (Fernandes et al., 2023; Hanbeyoglu-Akturk et al., 2025). When
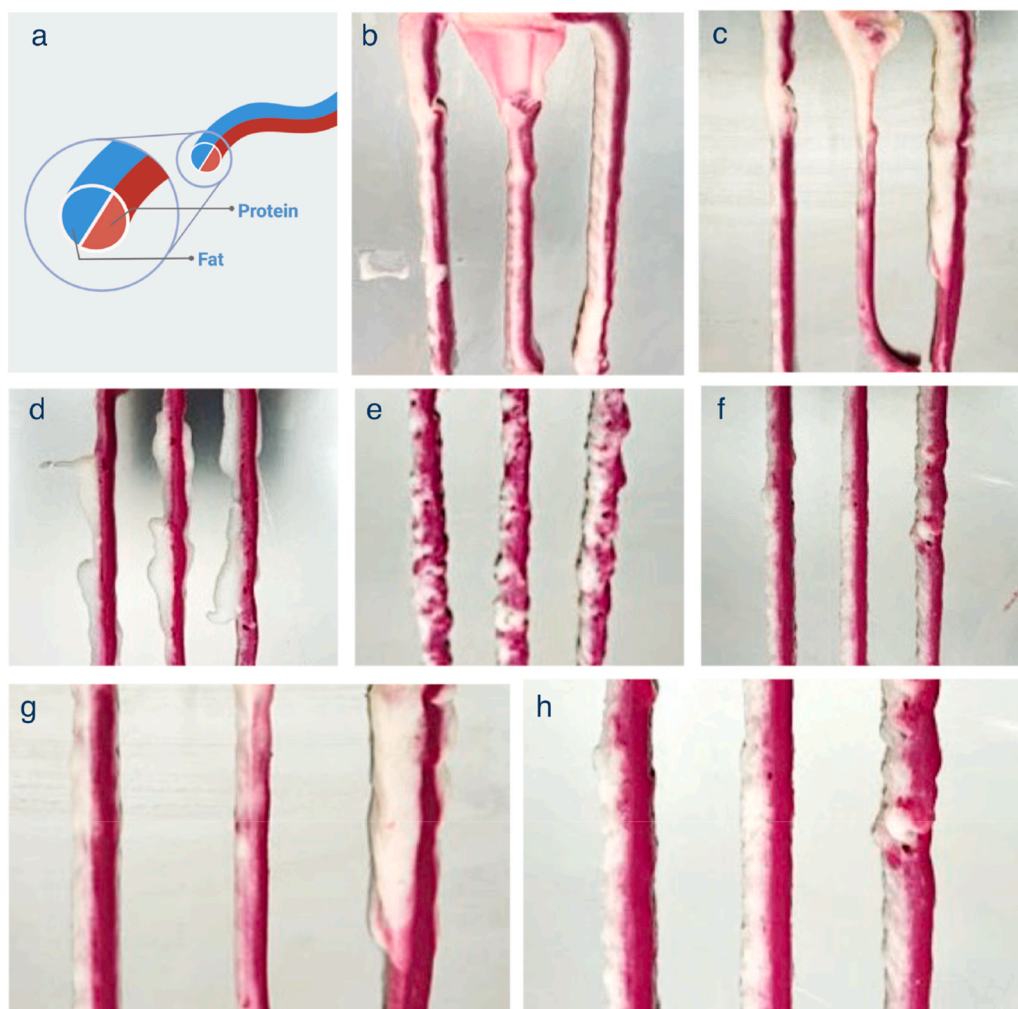
Fig. 7. Visual images from the line test in dual-extrusion, multi-phase 3D printing. (a) Schematic view showing the fat and protein phases; comparison of material distribution and compatibility using pea protein isolate with: (b) emulsion gel printed at 50 % speed, (c) emulsion gel at 20 % speed, (d) bigel printed at 60 °C and 100 % speed, (e) bigel at 40 °C and 100 % speed, (f) bigel at 40 °C and 50 % speed, (g) zoomed-in image of emulsion gel printed at at 50 % speed, and (h) bigel printed with pea protein isolate at 40 °C and 50 % speed.
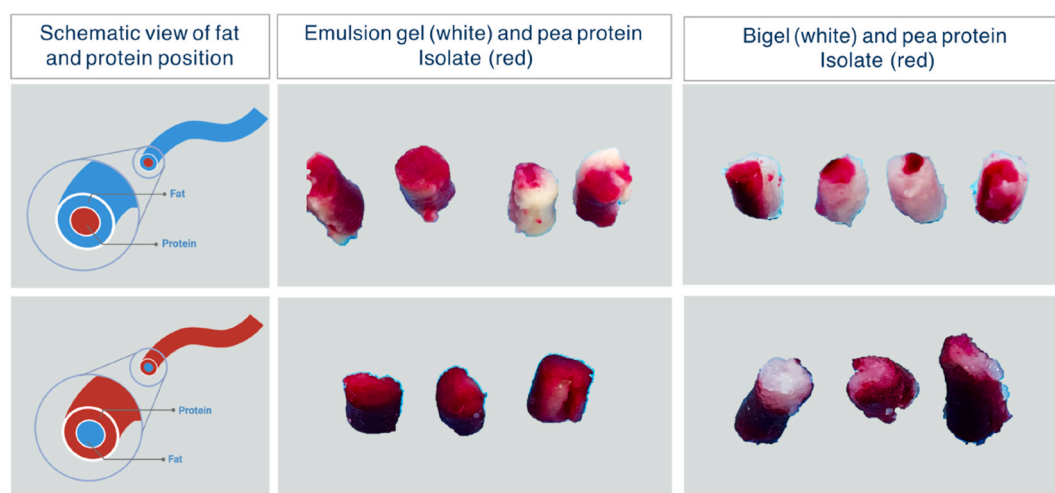

Fig. 8. Results from multi-material 3D printing using the coaxial extrusion mode, illustrating the impact of material composition on core-shell structure formation. The colored circles indicate the configurations for each sample, where the white color represents the fat gels and the pink is pea protein isolate. (For interpretation of the references to color in this figure legend, the reader is referred to the Web version of this article.)

printed at 60 °C, the results in Fig. 7d, revealed that the 4 mm nozzle caused the material to be extruded too quickly in comparison with the 1 mm nozzle, causing the material to be extruded at a too liquid state. This aligns with the observations in Supplementary Fig. 4, where the impact of the printing temperature on printability was evident. At 100 % speed, displayed in Fig. 7e, material compatibility was improved, while still exhibiting certain irregularities in material distribution across the lines. Furthermore, 50 % speed resulted in a much smoother distribution, exhibiting a close to 50:50 ratio across the entire strands, see Fig. 7f.

The emulsion gel showed less defined phase separation, with more irregular mixing and inconsistent distribution along the strands, reflecting its softer nature. In contrast, the bigel demonstrates clearer material separation, more consistent distribution, and better material compatibility. These differences highlight the influence of internal network strength and viscosity on the multi-material print quality. These results align with earlier reports on MM3DP, where internal gel strength and rheological robustness were shown to be critical determinants of material–material fidelity in composite prints (Caron et al., 2024; Lee et al., 2024; Y. Wang et al., 2025)

The coaxial printing trials further underscored the superiority of the bigel formulation. The bigel again outperformed the emulsion gel, maintaining clear core-shell structures with distinct boundaries as seen in Fig. 8. This performance reflects the bigel's higher elastic modulus and its ability to withstand radial shear stress during coaxial extrusion. The emulsion gel, however, failed to form continuous outer shells, resulting in uneven distribution and phase blending with the core material. These results again highlight the lower cohesiveness and poor extrusion stability of the emulsion gel, likely due to weak inter-droplet interactions and lack of a percolated gel network capable of supporting axial alignment under flow (Dickinson, 2012, 2013). The comparative performance between emulsion gel and bigel in MM3DP emphasizes the critical role of internal gel network architecture in determining printability, material compatibility, and spatial resolution in structured food applications. The bigel's biphasic structure not only provides mechanical support during deposition but also promotes stable interfacial contact with co-printed materials like PPI. This is consistent with the rheological findings, showing that the bigel's higher G' and more cohesive internal structure make it better suited for MM3DP. Overall, these results highlight the advantages of bigel for MM3DP, while also

indicating the need for further optimization of the emulsion gel to improve its printability and compatibility with other materials.

3.5. Confocal laser scanning microscopy of multi-material 3D printed gels

To further evaluate material–material interactions and the structural fidelity of multi-material 3D printing (MM3DP), CLSM analysis was performed on dual-extruded strands of emulsion gel–PPI and bigel–PPI systems. This provided microstructural insight on how each gel interfaces with pea protein isolate during co-deposition. As shown in the CLSM micrographs (Fig. 9), the emulsion gel–PPI interface exhibited diffuse boundaries, with visible blending of the fluorescently labeled phases. The transition zone between the gel and PPI was irregular, often lacking a clear demarcation. This suggests that the emulsion gel network was not able to sustain a sharp material interface under shear and deposition stress. Such interfacial smearing is consistent with the earlier macroscopic observations of smudging and phase mixing (Fig. 7) and indicates low interfacial stability, likely resulting from the emulsion gel's softer structure, lower G', and weaker internal cohesion.

In contrast, the CLSM images of the bigel–PPI interface showed much sharper and more continuous phase boundaries, with the bigel retaining its structure and forming distinct adjacent layers alongside the protein matrix. The images clearly delineate the two materials, indicating minimal interdiffusion at the microstructural level. This can be attributed to the enhanced network strength of the bigel, which consists of a biphasic combination of an oleogel and a hydrogel. Such architecture contributes to its improved mechanical robustness and extrusion fidelity, enabling it to better withstand shear forces and maintain material separation during deposition.

These findings underscore the importance of internal gel architecture in controlling interfacial behavior in MM3DP. The emulsion gel, lacking a percolated or reinforced matrix, behaves more like a soft colloidal fluid under stress, which leads to interpenetration at the interface with more solid-like materials such as PPI. In contrast, the bigel forms an interpenetrating network, which has been shown in previous studies to provide both elastic recovery and structural rigidity, minimizing unwanted blending at contact zones (Qiu et al., 2022; Zampouni et al., 2024). Moreover, the smooth and well-defined interface observed in the bigel system is crucial for the development of layered or
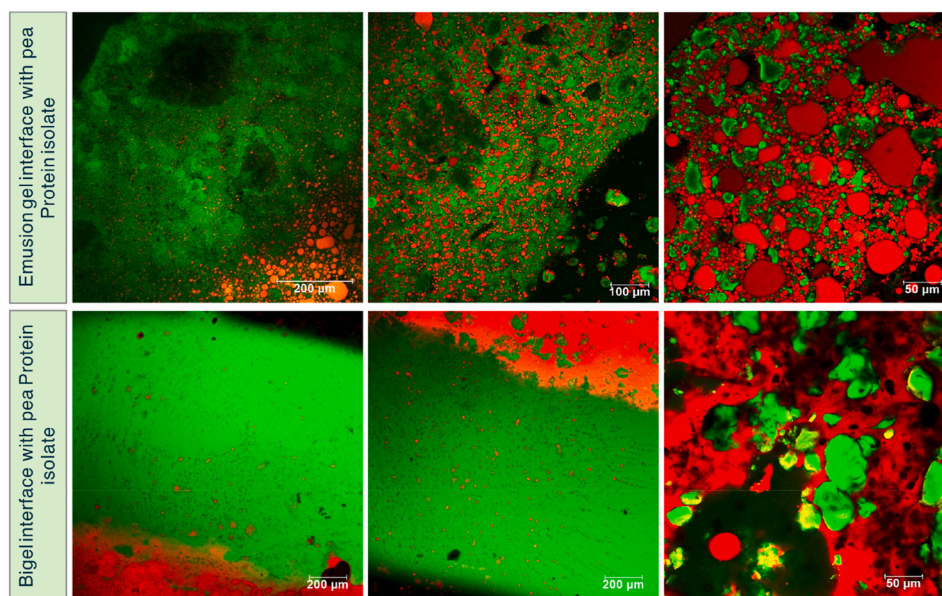

Fig. 9. Confocal Laser Scanning Microscopy (CLSM) micrographs showing the interfacial structure between pea protein isolate (PPI) (green) and emulsion gel (protein phase green, oil red) and bigel (hydrogel green, oleogel red) in dual extrusion multi-material 3D printing. (For interpretation of the references to color in this figure legend, the reader is referred to the Web version of this article.)

gradient-structured foods, where phase separation and compartmentalization are essential for sensory differentiation and controlled texture or nutrient release. These CLSM results strongly support the macro-scale printability trends observed earlier and highlight that print fidelity is not only governed by external extrusion parameters but also by microstructural compatibility between materials. For MM3DP to succeed in food applications, the formulation must strike a balance between printability, mechanical integrity, and phase stability at the material, material interface. Optimizing the interfacial behavior of emulsion gels—e.g., by increasing network strength, adding structuring agents, or improving emulsion droplet packing, could enhance their future use in co-printing applications. Additionally, CLSM imaging proves to be a powerful diagnostic tool for validating the structural performance of printed food constructs at the microscopic level.

4. Conclusions

The printability, buildability, and material compatibility of emulsion gels and bigels for extrusion-based 3D food printing in side-by-side single-material and subsequently in multi-material 3D printing (MM3DP) with pea protein isolate were comprehensively assessed. Rheological characterization revealed that bigels exhibited significantly ($p < 0.05$) higher storage modulus (G') of approximately 1200 KPa at 25 °C, nearly three times higher than that of emulsion gels (10 KPa) and yield stress (515 Pa vs 238 Pa) compared to emulsion gels, indicating a stronger and more elastic internal network. This directly translated into superior printability and structural integrity during 3D printing. In single-material printing, the bigel maintained high shape fidelity, especially at 40 °C, while the emulsion gel began to exhibit loss of structure above 50 °C, aligning with its lower storage modulus and more fluid-like behavior. Increasing the layer height further challenged printability, particularly for the emulsion gel, which failed to sustain vertical buildability, whereas the bigel retained better buildability due to its higher viscosity and yield stress. Confocal laser scanning microscopy (CLSM) micrographs confirmed that 3D printing preserved the internal microstructure of both gel systems, though some shear-induced reorganization was observed. In MM3DP, the emulsion gel displayed poor compatibility with the pea protein isolate, as evidenced by smearing, uneven extrusion, and random phase blending. These issues reflect its weaker viscoelastic structure and lower interfacial stability, further confirmed by its inability to maintain a consistent 50:50 distribution in dual-extrusion and core-shell integrity in coaxial extrusion, as shown by CLMS micrographs. In contrast, the bigel maintained clearer phase boundaries, more uniform co-deposition, and better core–shell structures, especially at lower speeds and temperatures, demonstrating greater interfacial cohesion and mechanical robustness. Overall, the study successfully demonstrated that bigels possess more favorable viscoelastic and interfacial properties for MM3DP applications. These results validate the hypothesis that gel network strength and structural design critically influence MM3DP outcomes. Emulsion gels, while printable in isolation, require reformulation (e.g., strengthening of the gel matrix or tuning interfacial behavior) to be effective in multi-material systems. These insights provide a foundation for the rational design of printable food matrices tailored for complex, multi-phase architectures in personalized and sustainable food production. Future work should investigate how the bigel system performs together with plant proteins in real food matrices, especially in terms of flavor release, juiciness, and after thermal processing.

CRediT authorship contribution statement

Linnea Johansson: Writing – review & editing, Writing – original draft, Visualization, Validation, Methodology, Investigation, Formal analysis, Data curation. **Isabel Badager:** Writing – review & editing, Validation, Supervision, Methodology, Formal analysis. **Annika Krona:** Writing – original draft, Visualization, Resources, Investigation. **Mehdi**

Abdollahi: Writing – review & editing, Visualization, Validation, Supervision, Resources, Project administration, Funding acquisition, Conceptualization.

Declaration of competing interest

The authors declare that they have no known competing financial interests or personal relationships that could have appeared to influence the work reported in this paper.

Appendix A. Supplementary data

Supplementary data to this article can be found online at https://doi.org/10.1016/j.foodhyd.2025.111964.

Data availability

Data will be made available on request.

References

Abdollahi, M., Nieuwland, M., van Bommel, K., Pouvreau, L., Ström, A., & Undeland, I. (2025). Texture engineering of aquatic protein-based products via 3D food printing. *Future Foods, 11*, 100604.

Appiani, M., Cattaneo, C., & Laureati, M. (2023). Sensory properties and consumer acceptance of plant-based meat, dairy, fish and eggs analogs: A systematic review. *Frontiers in Sustainable Food Systems, 7,* Article 1268068. https://doi.org/10.3389/FSUFS.2023.1268068/TEXT

Asyrul-Izhar, A. B., Bakar, J., Sazili, A. Q., Goh, Y. M., & Ismail-Fitry, M. R. (2023). Emulsion gels formed by electrostatic interaction of gelatine and modified corn starch via pH adjustments: Potential fat replacers in meat products. *Gels, 9*(1), 50. https://doi.org/10.3390/GELS9010050

Bajželj, B., Laguzzi, F., & Röös, E. (2021). The role of fats in the transition to sustainable diets. *The Lancet Planetary Health, 5*(9), e644–e653. https://doi.org/10.1016/S2542-5196(21

Caron, E., Van de Walle, D., Dewettinck, K., & Marchesini, F. H. (2024). State of the art, challenges, and future prospects for the multi-material 3D printing of plant-based meat. *Food Research International, 192*, Article 114712. https://doi.org/10.1016/J.FOODRES.2024.114712

Cen, S., Li, S., & Meng, Z. (2024). Advances of protein-based emulsion gels as fat analogues: Systematic classification, formation mechanism, and food application. *Food Research International, 191*, Article 114703. https://doi.org/10.1016/J.FOODRES.2024.114703

Cen, S., & Meng, Z. (2024). Advances of plant-based fat analogs in 3D printing: Manufacturing strategies, printabilities, and food applications. *Food Research International, 197*, Article 115178. https://doi.org/10.1016/J.FOODRES.2024.115178

Chao, E., Li, J., Duan, Z., & Fan, L. (2024). Bigels as emerging biphasic systems: Properties, applications, and prospects in the food industry. *Food Hydrocolloids, 154*, Article 110089. https://doi.org/10.1016/J.FOODHYD.2024.110089

Chen, Q., Chen, Z., Zhang, J., Wang, Q., & Wang, Y. (2023). Application of lipids and their potential replacers in plant-based meat analogs. *Trends in Food Science & Technology, 138*, 645–654. https://doi.org/10.1016/J.TIFS.2023.07.007

Czapalay, E., & Marangoni, A. (2024). Functional properties of oleogels and emulsion gels as adipose tissue mimetics. *Trends in Food Science & Technology, 153*, Article 104753. https://doi.org/10.1016/J.TIFS.2024.104753

Dickinson, E. (2012). Emulsion gels: The structuring of soft solids with protein-stabilized oil droplets. *Food Hydrocolloids, 28*(1), 224–241. https://doi.org/10.1016/J.FOODHYD.2011.12.017

Dickinson, E. (2013). Stabilising emulsion-based colloidal structures with mixed food ingredients. *Journal of the Science of Food and Agriculture, 93*(4), 710–721. https://doi.org/10.1002/JSFA.6013

Fernandes, A. S., Neves, B. V., Mazzo, T. M., Longo, E., Jacob-Lopez, E., Zepka, L. Q., & de Rosso, V. V. (2023). Bigels as potential inks for extrusion-based 3d food printing: Effect of oleogel fraction on physical characterization and printability. *Food Hydrocolloids, 144*, Article 108986. https://doi.org/10.1016/J.FOODHYD.2023.108986

Godoi, F. C., Prakash, S., & Bhandari, B. R. (2016). 3d printing technologies applied for food design: Status and prospects. *Journal of Food Engineering, 179*, 44–54. https://doi.org/10.1016/J.JFOODENG.2016.01.025

Gu, X., Cui, L., & Meng, Z. (2023). Differences of wax-based emulsion gel in 3D printing performance: Crystal distribution and droplet stability. *Food Chemistry, 428*, Article 136760. https://doi.org/10.1016/j.foodchem.2023.136760

Hanbeyoglu-Akturk, G., Demircan, E., & Ozcelik, B. (2025). Printability of bigel inks as fat analogs: Impact of gelators on structure. *Journal of Food Engineering, 400*, Article 112654. https://doi.org/10.1016/j.jfoodeng.2025.112654

Hashemi, B., Assadpour, E., Wang, Y., & Jafari, S. M. (2025). Pickering emulsion gels stabilized by protein and polysaccharide-based particles: A review of stability, synthesis, applications and prospective. *Advances in Colloid and Interface Science, 343*, Article 103564. https://doi.org/10.1016/J.CIS.2025.103564

Jiang, H., Zheng, L., Zou, Y., Tong, Z., Han, S., & Wang, S. (2019). 3D food printing: Main components selection by considering rheological properties. *Critical Reviews in Food Science and Nutrition, 59*(14), 2335–2347. https://doi.org/10.1080/10408398

Lee, C. P., Ng, M. J. Y., Chian, N. M. Y., & Hashimoto, M. (2024). Multi-material direct ink writing 3D food printing using multi-channel nozzle. *Future Foods, 10*, Article 100376. https://doi.org/10.1016/J.FUFO.2024.100376

Lille, M., Nurmela, A., Nordlund, E., Metsä-Kortelainen, S., & Sozer, N. (2018). Applicability of protein and fiber-rich food materials in extrusion-based 3D printing. *Journal of Food Engineering, 220*, 20–27. https://doi.org/10.1016/J.JFOODENG.2017.04.034

Liu, X., Cheng, Y., Sun, T., Lu, Y., Huan, S., Liu, S., Li, W., Li, Z., Liu, Y., Rojas, O. J., McClements, D. J., & Bai, L. (2025). Recent advances in plant-based edible emulsion gels for 3D-Printed foods. *Annual Review of Food Science and Technology, 16*(1), 63–79. https://doi.org/10.1146/annurev-food-111523-121736

Outrequin, T. C. R., Gamonpilas, C., Siriwatwechakul, W., & Sreearunothai, P. (2023). Extrusion-based 3D printing of food biopolymers: A highlight on the important rheological parameters to reach printability. *Journal of Food Engineering, 342*, Article 111371. https://doi.org/10.1016/j.jfoodeng.2022.111371

Patel, A. R. (Ed.). (2017). *Edible oil structuring: Concepts, methods and applications*. https://doi.org/10.1039/9781788010184

Pulatsu, E., & Lin, M. (2021). A review on customizing edible food materials into 3D printable inks: Approaches and strategies. *Trends in Food Science & Technology, 107*, 68–77. https://doi.org/10.1016/J.TIFS.2020.11.023

Qiu, R., Qiu, G., Zhao, P., Awais, M., Fan, B., Huang, Y., Tong, L., Wang, L., Liu, L., & Wang, F. (2024). Regulation of rheological properties of soy protein isolate-beeswax based bigel inks for high-precision 3D printing. *Food Hydrocolloids, 153*, Article 110052. https://doi.org/10.1016/J.FOODHYD.2024.110052

Qiu, R., Wang, K., Tian, H., Liu, X., Liu, G., Hu, Z., & Zhao, L. (2022). Analysis on the printability and rheological characteristics of bigel inks: Potential in 3D food printing. *Food Hydrocolloids, 129*, Article 107675. https://doi.org/10.1016/J.FOODHYD.2022.107675

Sajib, M., Forghani, B., Vate, N. K., & Abdollahi, M. (2023). Combined effects of isolation temperature and pH on functionality and beany flavor of pea protein isolates for meat analogue applications. *Food Chemistry, 412*, 135585.

Shakeel, A., Farooq, U., Gabriele, D., Marangoni, A. G., & Lupi, F. R. (2021). Bigels and multi-component organogels: An overview from rheological perspective. *Food Hydrocolloids, 111*, Article 106190. https://doi.org/10.1016/J.FOODHYD.2020.106190

Sinha, S. S., Upadhyay, A., Singh, A., Mishra, S., & Pandey, N. (2024). Bigels a versatile gel composite for tailored application in food industries: A review. *Food Structure, 41*, Article 100380. https://doi.org/10.1016/J.FOOSTR.2024.100380

Szenderák, J., Fróna, D., & Rákos, M. (2022). Consumer acceptance of plant-based meat substitutes: A narrative review. *Foods, 11*(9), 1274. https://doi.org/10.3390/FOODS11091274/S1

Tang, T., Zhang, M., Bhandari, B., & Li, C. (2024). Personalized transformation of 3D printing for traditional multi-material food with stuffing:a review. *Food Bioscience, 59*, Article 104112. https://doi.org/10.1016/J.FBIO.2024.104112

Torres, M. D. (2017). Editorial OMICS international role of the rheology in the new emerging technologies as 3D printing. https://www.omicsonline.org/open-access/role-of-the-rheology-in-the-new-emerging-technologies-as-3d-printing.pdf.

Vershkov, B., & Davidovich-Pinhas, M. (2023). The effect of preparation temperature and composition on bigel performance as fat replacers. *Food & Function, 14*(8), 3838–3848. https://doi.org/10.1039/D3FO00002H

Wang, Y., Ge, Z., Li, L., Gao, Y., Lai, K. hung, & Cai, W. (2025). Multimaterial 3D printing of plant protein-based material. *Innovative Food Science & Emerging Technologies, 100*, Article 103901. https://doi.org/10.1016/J.IFSET.2024.103901

Villacís-Chiriboga, J., Sharifi, E., Elíasdóttir, H. G., Huang, Z., Jafarzadeh, S., & Abdollahi, M. (2025). Hybrid plant-based meat alternatives structured via co-extrusion: A review. *Trends in Food Science & Technology*, 105013.

Wang, C., Yan, R., Li, X., Sang, S., McClements, D. J., Chen, L., Long, J., Jiao, A., Wang, J., Qiu, C., & Jin, Z. (2023). Development of emulsion-based edible inks for 3D printing applications: Pickering emulsion gels. *Food Hydrocolloids, 138*, Article 108482. https://doi.org/10.1016/J.FOODHYD.2023.108482

Wen, Y., Chao, C., Che, Q. T., Kim, H. W., & Park, H. J. (2023). Development of plant-based meat analogs using 3D printing: Status and opportunities. *Trends in Food Science & Technology, 132*, 76–92. https://doi.org/10.1016/J.TIFS.2022.12.010

Xiong, T., Sun, H., Niu, Z., Xu, W., Li, Z., He, Y., Luo, D., Xi, W., Wei, J., & Zhang, C. (2022). Carrageenan-based pickering emulsion gels stabilized by xanthan gum/lysozyme nanoparticle: Microstructure, rheological, and texture perspective. *Foods, 11*(23). https://doi.org/10.3390/FOODS11233757

Zampouni, K., Dimakopoulou-Papazoglou, D., & Katsanidis, E. (2024). Food-grade bigel systems: Formulation, characterization, and applications for novel food product development. *Gels, 10*(11), 712. https://doi.org/10.3390/GELS10110712

Zhong, Y., Wang, B., Lv, W., Wu, Y., Lv, Y., & Sheng, S. (2024). Recent research and applications in lipid-based food and lipid-incorporated bioink for 3D printing. *Food Chemistry, 458*, Article 140294. https://doi.org/10.1016/J.FOODCHEM.2024.140294

Zhu, P., Chu, Y., Yang, J., & Chen, L. (2024). Thermally reversible emulsion gels and high internal phase emulsions based solely on pea protein for 3D printing. *Food Hydrocolloids, 157*, Article 110391. https://doi.org/10.1016/J.FOODHYD.2024.110391